nature astronomy

LETTERS

https://doi.org/10.1038/s41550-018-0664-0

Detailed polarization measurements of the prompt emission of five gamma-ray bursts

Shuang-Nan Zhang[1,2,10*], Merlin Kole[3,10*], Tian-Wei Bao[1], Tadeusz Batsch[4], Tancredi Bernasconi[5], Franck Cadoux[3], Jun-Ying Chai[1,2], Zi-Gao Dai[6,7], Yong-Wei Dong[1], Neal Gauvin[5], Wojtek Hajdas[8], Mi-Xiang Lan[6,9], Han-Cheng Li[1,2], Lu Li[1], Zheng-Heng Li[1,2], Jiang-Tao Liu[1], Xin Liu[1,2], Radoslaw Marcinkowski[8], Nicolas Produit[5], Silvio Orsi[3], Martin Pohl[3], Dominik Rybka[4], Hao-Li Shi[1], Li-Ming Song[1,2], Jian-Chao Sun[1], Jacek Szabelski[4], Teresa Tymieniecka[4], Rui-Jie Wang[1], Yuan-Hao Wang[1,2], Xing Wen[1,2], Bo-Bing Wu[1], Xin Wu[3], Xue-Feng Wu[9], Hua-Lin Xiao[1,8], Shao-Lin Xiong[1], Lai-Yu Zhang[1], Li Zhang[1], Xiao-Feng Zhang[1], Yong-Jie Zhang[1] and Anna Zwolinska[4]

Gamma-ray bursts (GRBs) are the strongest explosions in the Universe since the Big Bang. They are believed to be produced either in the formation of black holes at the end of massive star evolution[1-3] or the merging of compact objects[4]. Spectral and timing properties of GRBs suggest that the observed bright gamma-rays are produced in the most relativistic jets in the Universe[4]; however, the physical properties (especially the structure and magnetic topologies) of the jets are still not well known, despite several decades of studies. It is widely believed that precise measurements of the polarization properties of GRBs should provide crucial information on the highly relativistic jets[5]. As a result, there have been many reports of GRB polarization measurements with diverse results (see ref. [6]); however, many such measurements suffer from substantial uncertainties, most of which are systematic (ref. [7] and the references therein). After the first successful measurements by the Gamma-Ray Burst Polarimeter (GAP) and Compton Spectrometer and Imager (COSI) instruments[8-10], here we report a statistically meaningful sample of precise polarization measurements, obtained with the dedicated GRB polarimeter POLAR onboard China's Tiangong-2 space laboratory. Our results suggest that the gamma-ray emission is at most polarized at a level lower than some popular models have predicted, although our results also show intrapulse evolution of the polarization angle. This indicates that the low polarization degrees could be due to an evolving polarization angle during a GRB.

POLAR is a dedicated gamma-ray burst (GRB) polarization detection experiment onboard China's Tiangong-2 space laboratory[11]. It was launched on 15 September 2016 and stopped operation on 31 March 2017. POLAR detected 55 GRBs with high significance. To make statistically significant GRB polarization measurements with negligible systematic errors, we select a subsample of five GRBs for detailed analysis of their polarization properties (see the Supplementary Information for the sample selection criteria and properties of the five selected GRBs). We employ a straightforward χ^2-based analysis, similar to that successfully employed in ref. [10], to study the polarization properties of the five GRBs, while a Bayesian method is employed to accurately determine the credible regions of the measurements. The studies rely on extensive ground and in-orbit calibration data and Monte Carlo simulations matching the calibration data[12,13]. Please refer to the Methods for details of the methodology and analysis.

In Fig. 1, we show the measured modulation curves of the five GRBs integrated over the whole GRB duration, together with the best-fitting simulated modulation curves from linear polarization and fitting residuals. All fittings are statistically acceptable, with no significant systematic deviations. In Fig. 2, we show the two-dimensional (2D) posterior distributions of the five GRBs (that is, the posterior probability as functions of both the polarization angle and polarization degree). Clearly, the measured polarization degree is correlated with the polarization angle for all five GRBs. We therefore calculate the cumulative probabilities of the polarization degree marginalized over the polarization angle for all five GRBs, as shown in Fig. 3. In Table 1, we summarize the main results for the five GRBs, including for each its name, T_{90} value[14] (the time interval over which 90% of the total background-subtracted counts are observed), fluence, most likely polarization degree value, compatibility of the time-integrated polarization with an unpolarized flux, upper limit of the polarization degree, most likely polarization angle, and evidence for a change in the polarization angle.

We conclude that for the polarization degree measurement, the most probable polarization degree values for all five GRBs are between 4 and 11%. The 99% upper limit ranges between 28 and 45% for four GRBs and is 67% for GRB 170127C, which has the lowest fluence and thus the poorest statistics for polarization measurement. Although the analysis provides non-zero polarization degree values, it should be noted that linear polarization measurements always provide positive results (see, for example, ref. [15] and the references therein for a discussion). The low polarization degrees

[1]Key Laboratory of Particle Astrophysics, Institute of High Energy Physics, Chinese Academy of Sciences, Beijing, China. [2]University of Chinese Academy of Sciences, Beijing, China. [3]Department of Nuclear and Particle Physics, University of Geneva, Geneva, Switzerland. [4]National Centre for Nuclear Research, Otwock, Poland. [5]ISDC/Geneva Observatory, University of Geneva, Versoix, Switzerland. [6]School of Astronomy and Space Science, Nanjing University, Nanjing, China. [7]Key Laboratory of Modern Astronomy and Astrophysics (Nanjing University), Ministry of Education, Nanjing, China. [8]Paul Scherrer Institut, Villigen, Switzerland. [9]Purple Mountain Observatory, Chinese Academy of Sciences, Nanjing, China. [10]These authors contributed equally: Shuang-Nan Zhang, Merlin Kole. *e-mail: zhangsn@ihep.ac.cn; merlin.kole@unige.ch

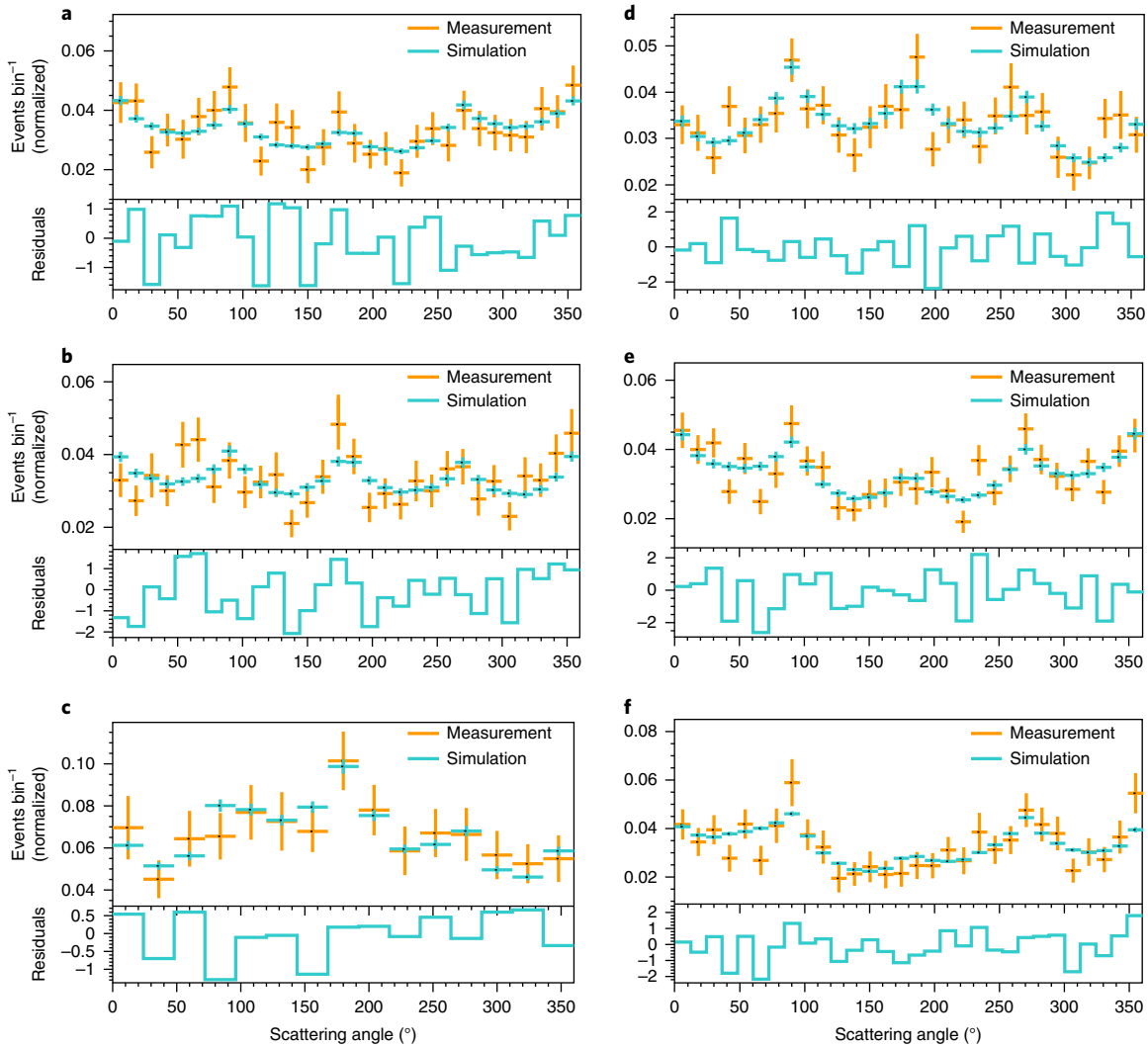

Fig. 1 | Measured and best-fitting simulated modulation curves for all five GRBs and the second time interval of GRB 170114A. Orange crosses are the measured modulation curves normalized to have a total bin content of unity, after subtracting the background. The uncertainties in the orange histograms contain the statistical uncertainties. A grid of 6,060 equally normalized simulated modulation curves is produced with different values for the polarization degree and angle. The blue crosses are the Monte Carlo-produced modulation curves best fitting the measured data, and the uncertainties displayed here contain both the statistical and systematic uncertainties. The blue histograms below are the fitting residuals. **a**, 161218A. **b**, 170101A. **c**, 170127C. **d**, 170206A. **e**, 170114A. **f**, Second half (3 s) of 170114A. The detailed fitting results are listed in Table 1.

found in the analysis presented here do not allow us to fully reject the hypothesis that every GRB is non-polarized. However, from Fig. 3, we can find for each GRB the probability that the polarization degree is less than a certain positive value, which turns out to be between 5.8 and 14% for the 2% polarization degree. Since all five GRBs show statistically consistent polarization degrees, we can combine the measurements to give joint lower and upper limits. As can be seen in Fig. 3f, the average polarization degree is 10% and the probability that the polarization degrees of all the five GRBs are lower than 5% or higher than 16% is 0.1%. Our results indicate with high precision that the prompt gamma-ray emission of GRBs is not highly polarized, as some models have predicted. Furthermore, the results favour a low polarization level and can reject the hypothesis that all GRBs are unpolarized, while several individual GRB polarization levels are still found to be consistent with zero polarization. Further evidence for low but non-zero polarization degree values was found when performing time-dependent analysis.

Previously, it has been reported that the polarization angle of GRBs can change during a GRB[10]. We thus divide each of the five GRBs into two equal time bins and make the same analysis, to examine whether the polarization angle changed during each burst. As shown in detail in the Methods, a significant polarization angle change was not observed for three GRBs and cannot be constrained for GRB 170127C due to low statistics, but was clearly detected for GRB 170114A. Interestingly, GRB 170114A is a single-pulse GRB and also has the lowest polarization degree (4%) among all five GRBs integrated over the entire GRB periods. Performing a time-resolved analysis, similar to that applied previously by the GAP collaboration on the long multi-peak GRB 100826A, we find that the polarization properties of this GRB are best described by a constant polarization degree of 28% with a polarization angle that changes significantly during three 2-s time bins. While the time-integrated analysis of this GRB is consistent with an unpolarized flux, the time-resolved analysis results in a polarization degree that is inconsistent with an unpolarized flux with a 99.7% confidence level. While the measurement results of GAP for GRB 100826A already showed strong evidence of changes in the polarization angle for different peaks inside a long GRB, the measurement of

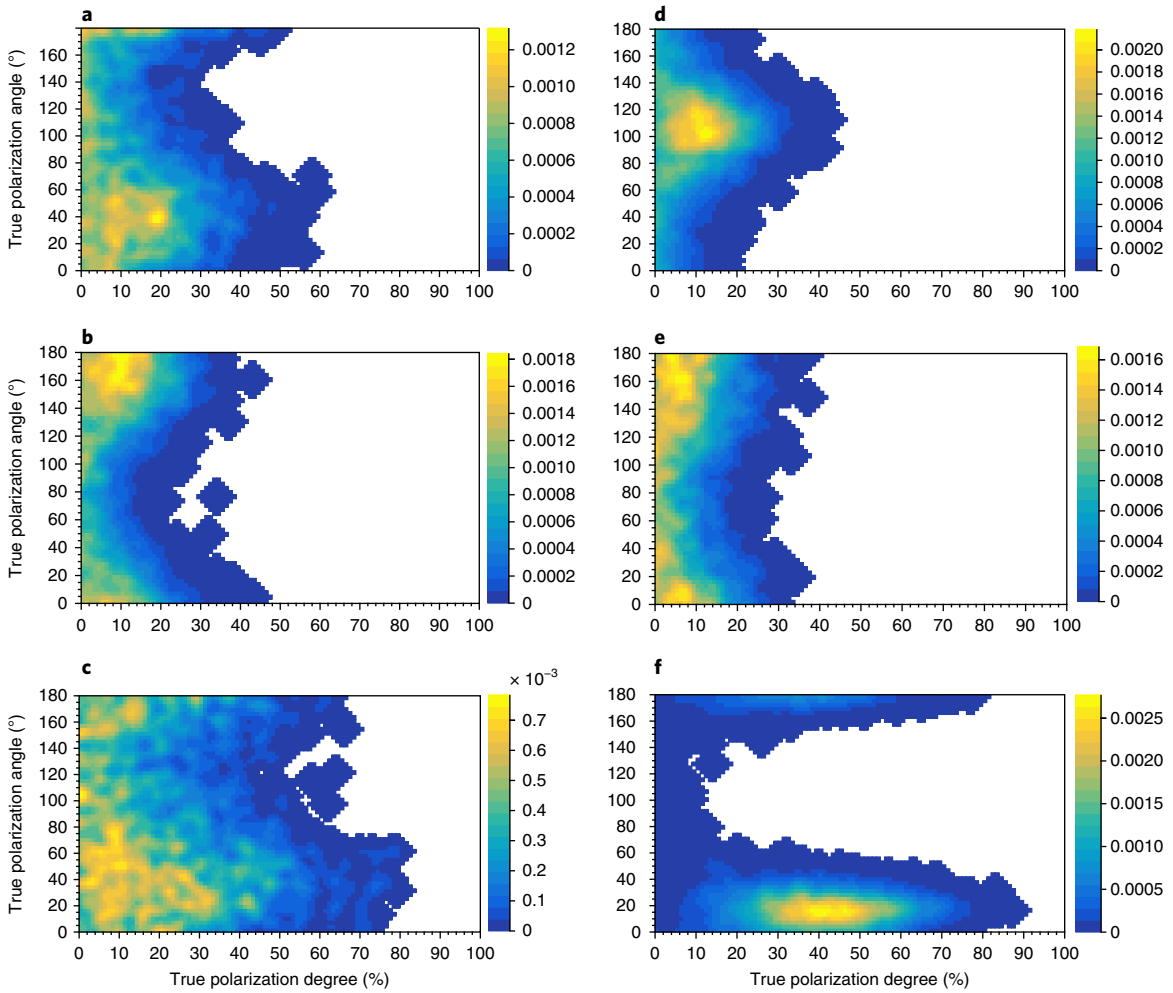

Fig. 2 | Posterior distributions of the polarization parameters for the five GRBs and the second time intervals of GRB 170114A. a, 161218A. **b**, 170101A. **c**, 170127C. **d**, 170206A. **e**, 170114A. **f**, Second half (3 s) of 170114A.

GRB 170114A shows an intrapulse evolution of the polarization angle. This implies that the measured low polarization degree for all GRBs in the sample presented here, integrated over the whole burst duration, might be due to rapid changes of polarization angle during the bursts. However, this cannot be well constrained with the current instruments.

In summary, with the dedicated GRB polarization instrument POLAR onboard China's Tiangong-2 space laboratory, we have measured the polarization properties of five GRBs with high precision. For the first time, we find that averaged over the whole bursts, GRBs are at most modestly polarized (that is, with a polarization degree of ~10%. For the brightest GRB in the sample, an unpolarized flux can be rejected using time-resolved analysis, and a polarization degree of $28 \pm 9\%$ is found. Furthermore, an intrapulse evolution of the polarization angle is detected, which has important implications for the time-integrated polarization degree measurements, as these low measurement values of the polarization degree of all GRBs might be due to rapid polarization angle changes during GRBs. Statistically, most previous prompt polarization emission measurements of GRBs, and some of quite high polarization degrees at face value, are consistent with our results, given their larger uncertainties in most cases. A summary of all previously reported GRB prompt emission polarization measurements is given in Supplementary Table 1.

Regarding the theoretical interpretation, there are three main factors that affect the polarization properties significantly: the emission mechanism[16–18], magnetic field configuration (MFC) (refs. [5,19,20] and the references therein) and jet geometry[21,22]. Several popular models have been proposed to interpret GRBs (for example, internal shock[23,24], dissipative photosphere[25,26] and internal-collision-induced magnetic reconnection and turbulence (ICMART)[27]). Depending on the MFC in the collision shell, the predicted polarization degree of the internal shock model can vary from a few percent to 70% (the PD of the mixed MFC can vary down to about 10%, and that of the large-scale ordered MFC can vary up to about 70%). For the dissipative photosphere model, the predicted polarization degree is relatively low in the gamma-ray band[28]. A decaying polarization degree is predicted during each pulse in the ICMART model (the maximum value at the beginning of the pulse can reach up to 60% and the minimum value at the end decreases to between a few percent and ~10%, as presented in ref. [27]). However, the detailed numerical simulations show that a polarization degree of ~10% is also possible for the ICMART model[29]. As our results show a relatively low polarization degree overall, at first sight they appear to agree with the dissipative photosphere model. However, this model has difficulty explaining the polarization degree of 28% detected for GRB 170114A using the time-binned analysis as well as the change in polarization angle, which appears to be of a continuous nature. The average polarization degree level of 10% is possible according to the ICMART model, depending on the MFC in the emission region. For the internal shock model, the predicted polarization degree can range from a few percent to 70%, depending on the MFC in the collision shells. The observed polarization degree of ~10% with POLAR

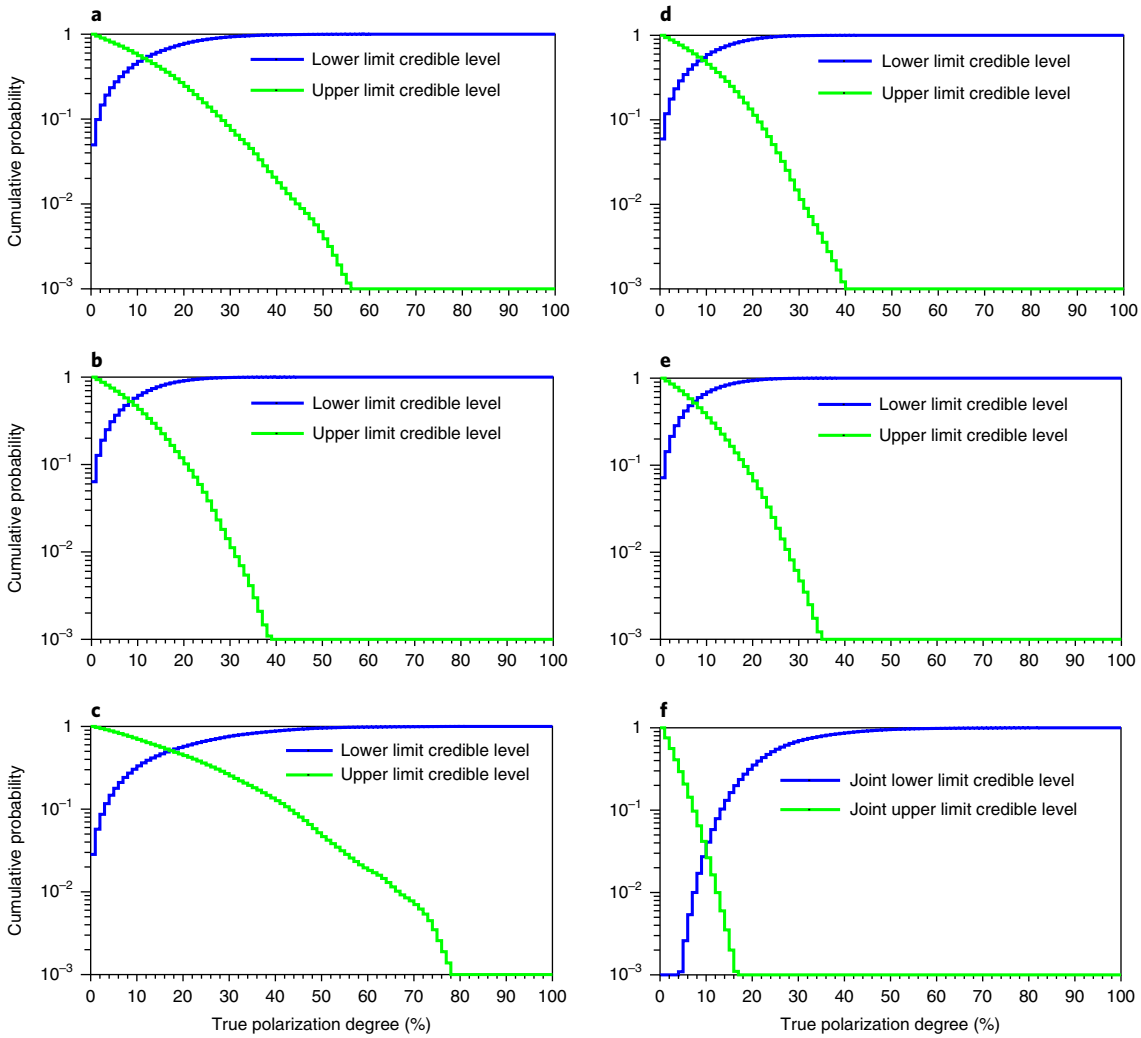

Fig. 3 | Cumulative probability functions of the polarization degree for the studied GRBs in this sample. Lower (blue) and upper (green) credible levels of the polarization degree of the five GRBs. **a**, 161218A. **b**, 170101A. **c**, 170127C. **d**, 170206A. **e**, 170114A. **f**, Joint lower and upper credible levels of the five GRBs. The lower credible level is the cumulative probability that the polarization degree is below the value given by the curve. The upper credible level is the cumulative probability that the polarization degree is above the value given by the curve. The joint lower or upper credible level of the five GRBs is the cumulative probability for all the five GRBs to be below or above the value given by the curve.

Table 1 | Summary of the five GRBs

GRB	T_{90} (s)	Fluence[a]	PD	Probability (PD < 2%)	PD_{up}(99%)	PA (°)	PA change
161218A	6.76	1.25×10^{-5}	9%	9%	45%	40	No
170101A	2.82	1.27×10^{-5}	8%	13%	31%	164	No
170127C	0.21	7.4×10^{-6}	11%	5.8%	67%	38	Unknown
170206A	1.2	1.34×10^{-5}	10%	12%	31%	106	No
170114A	8.0	1.93×10^{-5}	4%	14%	28%	164	Yes
170114Ap1	NA	NA	15%	8%	43%	122	NA
170114Ap2	NA	NA	41%	0.49%	74%	17	NA

The different properties of the five GRBs and two time bins of GRB 170114A are included. [a]In units of erg cm^{-2} in the 10–1,000 keV energy range. NA, not applicable; PA, polarization angle; PD, polarization degree; PD_{up}(99%), the 99% confidence upper limit in PD.

suggests that the MFC is probably mixed during the GRB prompt phase. Alternatively, a violent change of the polarization angle can also result in a decrease of the time-integrated polarization degree, which should have significant implications for all GRB models. To further understand the physics and astrophysics of the most relativistic jets produced by the strongest explosions in the Universe, future GRB polarization instruments are required to provide time-resolved polarization properties of much larger samples of GRBs.

Methods

Sample selection. The GRBs analysed in this paper were selected from the POLAR GRB catalogue, presented in ref. [30], based on the following criteria:

- The GRB has been observed by detectors other than POLAR, and good measurement of both the spectrum and location are provided by other instruments.
- The fluence of the GRB, as provided by other instruments in the 10–1,000 keV energy range, exceeds 5×10^{-6} erg cm^{-2}.
- The incoming angle with respect to the POLAR instrument zenith, θ, is below 45°.

The first selection criterion minimizes the systematic errors in the polarization results induced by uncertainties in the spectrum and location of the GRB. The second and third criteria ensure a large number of events and a large modulation factor (M_{100}—the amplitude of the modulation measured for a 100% polarized flux) and therefore a high statistical significance of the measurement. The third criterion furthermore reduces the influence of photons scattered off the objects in the vicinity of POLAR, thereby removing additional systematic errors.

This selection resulted in the following six GRBs eligible for study: 161129A, 161218A, 170101A, 170114A, 170127C and 170206A. The light curves of these GRBs can be found at https://www.isdc.unige.ch/polar/lc/. As GRB 161129A was preceded by a large solar flare, it was not included in this work, as systematics induced by potential low-level irradiation from the last part of the flare require further study. The light curves of the five remaining GRBs are shown in Supplementary Fig. 1. In these light curves, only events are selected where at least two bars are above the trigger level, as only these events can be used for polarization studies. Details of the event selection including the trigger algorithm can be found in ref. [12]. The different time bins studied for GRB 170114A, which are discussed below, are indicated in panel f of Supplementary Fig. 1.

Methodology of GRB polarization analysis. A full and detailed instrument calibration of the POLAR detector in orbit was a prerequisite for this polarization study. These results are presented in ref. [12]. Polarization analysis is performed by producing one modulation curve from the measured data. This modulation curve is fitted to a simulated instrument response consisting of 6,060 simulated modulation curves to find the best-fitting polarization degree and polarization angle, as described in more detail below.

The simulated response is produced using the Monte Carlo software, as presented in ref. [13]. It should be noted that some updates to the Monte Carlo software have been implemented since the publication of ref. [13], based on a deeper analysis of the in-orbit data. These updates mainly concern the inclusion of a detailed mass model of the Tiangong-2 space laboratory, on which POLAR is mounted, and a better parameterization of the nonlinearity of the energy gain based on the findings presented in ref. [12]. The measured and simulated data are processed using the methods described in ref. [12].

The event selection, as well as the processing of both the measured and simulated data, is equivalent. Events selected for analysis consist of all of the clean events, as described in ref. [12]. Additionally, no channels with an energy deposition above overflow are selected. Finally, the two channels in POLAR with the highest energy depositions, as measured in keV, are selected. The angle between the two bars is taken to be the scattering angle. The first bar of the two is that with the highest energy deposition within the whole event. The second bar is selected as that with the highest energy deposition among those bars not adjacent to the first bar. If the second channel is not found with the non-adjacent criterion, the event is not selected. The non-adjacent criterion is used to improve M_{100} and reduce the influence of the fluctuations of crosstalk signals. To reduce the effect of the energy threshold non-uniformity, an additional energy threshold of 15 keV is applied in the event selection on the energy deposition of the second channel.

For the measured modulation curve, the selected signal time intervals are based on the T_{90} values measured by POLAR. The background time interval is selected as two time intervals that are, respectively, before and after the GRB, as described in more detail in the Supplementary Information and indicated in Supplementary Fig. 1. The modulation curve of the background is subtracted from the modulation curve produced using data in the selected signal time interval. Here, the relative difference between the length of the signal and background intervals is taken into account, as well as the error propagation for each bin. As the background is relatively stable, as illustrated in Supplementary Fig. 6, the influence of the background selection on the final results was found to be negligible in a dedicated study described in detail in the Supplementary Information. The results are summarized in Supplementary Tables 2 and 3.

For each GRB, a range of simulations is performed. In each, the GRB is simulated using photons emitted from a circular plane with a radius of 250 mm, with the incident direction calculated based on the best available measured location for the GRB from other instruments. The influence of systematic uncertainties in the location of the GRB on our final results was found to be small through a dedicated study described in the Supplementary Information. Its results are summarized in Supplementary Table 5. The size of the emitting plane is sufficient to illuminate the full instrument, as well as the materials surrounding POLAR. It should furthermore be noted that it was found, by removing them in the simulations, that the materials surrounding POLAR have no significant influence on the final polarization measurement for the studied GRBs.

The energy spectrum of the simulated photons follows a Band function[31] using the best published parameters for the GRB. The influence of the choice of the used spectrum, when different spectra were available, was found to be negligible through a study described in the Supplementary Information. The results of this study are summarized in Supplementary Table 4. It should be noted here that the spectrum of GRB 170127C is best fitted using a single cut-off power-law and is therefore also modelled as such in the POLAR analysis. The lower limit for the energy range for simulated photons is 10 keV, below which the effective area of POLAR becomes negligible. The upper limit is set to 1,000 keV for all GRBs except 170127C, where this is extended up to 1,500 keV. At this level, according to the spectra provided by the Fermi-Gamma-ray Burst Monitor (GBM), the flux drops below 1% of that at 10 keV. The photons are then simulated with an origin from a random position in the circular plane and a momentum vector based on the GRB location with respect to POLAR. For each GRB, a total of 61 simulations are performed, each with 5 million photons. A total of 60 simulations are performed for the 100% polarized photons, differing in the polarization angles with step sizes of 3°. One simulation is performed for the unpolarized photons. The modulation curves of the polarization degrees between 0 and 100% can be generated by mixing those of the unpolarized flux and the 100% polarized flux. Therefore, using the modulation curves of the 61 simulations, a total of 6,060 different simulated modulation curves was generated in the 2D plane of the polarization angle and polarization degree, with steps of 1% in the polarization degree direction and 3° in the polarization angle direction. The modulation curves produced this way, as well as those from the measured data, are normalized by the total number of events within the modulation curve. Subsequently the 60×101 array of simulated modulation curves is used to find the best-fitted polarization angle and polarization degree for the measured modulation curve using the least χ^2 method, as discussed below. This array of simulated modulation curves is also used for the Bayesian analysis method, as discussed below, to generate the posterior probability distribution of the true polarization angle and polarization degree.

The results of this analysis when applied on full GRBs are detailed in Supplementary Table 7. The input parameters and their origins are summarized in Supplementary Table 6.

Least χ^2 analysis method. To determine the polarization angle and polarization degree of each GRB, the measured modulation curve is fitted with the simulated instrument response using the least χ^2 method. One χ^2 value between the measured modulation curve and one of the 6,060 simulated modulation curves, as mentioned above, can be calculated using equation (1):

$$\chi^2=\sum_{i=1}^{n}\frac{(X_i-Y_i)^2}{\varepsilon_i^2+\sigma_i^2} \quad (1)$$

where X_i and Y_i are the counts of the bins of the measured and simulated modulation curves, respectively, ε_i^2 and σ_i^2 are the uncertainties of X_i and Y_i, respectively, and n is the number of bins in the modulation curves. Note that both the measured and simulated modulation curves are normalized before calculating the χ^2 value. The uncertainties of the bins in the measured modulation curve are taken to be the statistical errors. On top of the statistical uncertainties in the simulated modulation curves, these also contain systematic uncertainties resulting both from the spectral and location parameters of the GRB as well as uncertainties in the calibration parameters used in the simulations. Details of the systematic error determination are described in the Supplementary Information.

Using the 6,060 simulated modulation curves and the single measured modulation curve with their corresponding errors, the 60×101 array of χ^2 values corresponding to different polarization angles and polarization degrees can be calculated. As an example, Supplementary Fig. 2 shows the map of $\Delta\chi^2=\chi^2-\chi^2_{\rm min}$ for GRB 170206A. The best-fitted polarization angle and polarization degree of this GRB are those corresponding to $\chi^2_{\rm min}$.

As discussed in ref. [32], the confidence area of the polarization angle–polarization degree measurement can be determined using the value of $\Delta\chi^2$. In Supplementary Fig. 2, the three black contours from left to right correspond to $\Delta\chi^2=2.28$, 4.61 and 9.21, which are the upper quantiles with probabilities 32, 10 and 1%, respectively, for the χ^2 distribution of 2 d.f. To get the upper limit of the polarization degree without considering the value of the polarization angle, the upper quantile of the 1 d.f. χ^2 distribution is used. The red contour corresponds to $\Delta\chi^2=6.64$, which is the upper quantile with a probability of 1% for the 1-d.f. χ^2 distribution. The maximum polarization degree on the red contour is the upper limit of the polarization degree with a confidence level of 99%, which is approximately 34%.

Bayesian analysis method. Suppose $\boldsymbol{A}=(\hat{p},\hat{\phi})$ is the measurement of the polarization degree and polarization angle using the least χ^2 method, as discussed in the previous section, and $\boldsymbol{B}_i=(p,\phi)$ is the true polarization degree and polarization angle of the source. Then, $P(\boldsymbol{A}|\boldsymbol{B}_i)$ is the probability that the measurement of the polarization degree and polarization angle is $\boldsymbol{A}$ under the

condition that the true polarization degree and polarization angle of the source is $\boldsymbol{B}_i$. If the prior probability of the true polarization degree and polarization angle of the source is $P(\boldsymbol{B}_i)$, the posterior probability of $\boldsymbol{B}_i$, under the condition that the measurement of the polarization degree and polarization angle is $\boldsymbol{A}$, can be acquired using the Bayesian equation as presented by equation (2):

$$P(\boldsymbol{B}_i \mid \boldsymbol{A}) = \frac{P(\boldsymbol{A} \mid \boldsymbol{B}_i) P(\boldsymbol{B}_i)}{\sum_{j=1}^{n} P(\boldsymbol{A} \mid \boldsymbol{B}_j) P(\boldsymbol{B}_j)} \quad (2)$$

Here, $P(\boldsymbol{A}|\boldsymbol{B}_i)$ for the different bins of $\boldsymbol{B}_i$ can be acquired by performing a series of measurement simulations, the procedure for which is described in the Supplementary Information. Some examples of the distribution of $P(\boldsymbol{A}|\boldsymbol{B}_i)$ for GRB 170206A are shown in Supplementary Fig. 3. As there is no information on the true polarization degree and polarization angle of the source before the measurement, the prior probability of $\boldsymbol{B}_i$ is taken to be uniform in the range 0–100% for the polarization degree and 0–180° for the polarization angle, and 0 outside these ranges. After producing the distribution of $P(\boldsymbol{A}|\boldsymbol{B}_i)$ for all different bins of $\boldsymbol{B}_i$, using simulations, the posterior probability distribution of the true polarization angle and polarization degree of the source under the condition of the single measurement can be directly calculated with equation (2). Supplementary Fig. 4 shows the result of $P(\boldsymbol{B}_i|\boldsymbol{A})$ for GRB 170206A, and Fig. 2 shows the results of all five selected GRBs.

After integrating the 2D posterior probability distribution of the polarization degree and polarization angle, as shown in Fig. 2 along the polarization angle direction, a one-dimensional posterior probability distribution of the polarization degree is acquired, as illustrated in Supplementary Fig. 5. This one-dimensional distribution can be used to find the upper limit of the polarization degree with a certain credible level by integrating it from right to left, and to find the lower limit by integrating it from left to right, as shown in Fig. 3. From Fig. 3b, it can be seen that the upper limit of the polarization degree with a credible level of 99% is about 31%, which is very similar to that obtained with the least χ^2 method.

Evolution of the polarization angle. For all GRBs with the exception of 170127C, which is too short and lacks statistics, a time-binned analysis is also performed. For this purpose, the data from the GRBs are split into equal time intervals. The GRBs 161218A, 170101A and 170206A are split into two intervals. GRB 170114A, which consists of a bright peak lasting approximately 6 s followed by 3 s with few events, is divided into 3 time bins. These time intervals for 170114A are indicated in Supplementary Fig. 1f. For this GRB, only the two time bins in the peak are discussed here as the minimum detectable polarization for the third bin is significantly larger than 100%, indicating that no constraining measurement on the polarization properties of this interval are possible.

The analysis is performed using two different approaches for each GRB. First, the data from both time bins are analysed independently following the same procedure as that applied in the analysis of the time-integrated GRBs. For the two time bins, the incoming angles as used in the simulations are corrected for the minor changes induced by the rotation of POLAR with respect to the GRB during the burst. The second applied method is the same as that used by the GAP collaboration for GRB 100826 (ref. [10]). In this analysis, the two time intervals are analysed simultaneously while the polarization degree of both intervals is forced to be equal, and the polarization angle is allowed to vary. This study therefore takes the assumption that the polarization degree is constant throughout the GRB, while the polarization angle can vary with time.

For GRBs 161218A, 170101A and 170206A, the analyses using both methods are found to give results for both time intervals that are consistent with the analysis of the full time-integrated GRB. No significant change in the angle is therefore found during these GRBs. However, it should be noted that this analysis is only performed when dividing the full GRB into two equal time intervals; we cannot exclude that the polarization angle varies on shorter time scales, since the data of POLAR lack the statistics to perform such studies.

For GRB 170114A, a significant evolution of the polarization angle is found using both analysis methods. In these analyses, the changes in the incoming angle of the GRB during the burst, as well as spectral evolution of the GRB, are taken into account. Such spectral evolution was not reported in the Gamma-ray Coordinates Network circular by Fermi-GBM[33]—the only other instrument apart from POLAR that reported a detection of this GRB. However, analysis of the Fermi-GBM data shows that a significant spectral evolution occurred during the GRB. Using independent analysis of both bins, and new spectra for the two time bins, resulted in the modulation curves presented in Supplementary Figs. 7 and 9, and the $\Delta\chi^2$ distributions shown in Supplementary Figs. 8 and 10. The first time interval is consistent with an unpolarized or lowly polarized flux and gives an upper limit of a polarization degree of 42%, while the second interval only has a 0.49% probability for a polarization degree lower than 2%. The 99% upper limit for the polarization degree of the second part is 74%.

Furthermore, it was found that the polarization degree of both time intervals is compatible within 1σ with a polarization degree around 25%, albeit with very different polarization angles. We can therefore perform the second analysis approach where the polarization degree for both bins is forced to be equal. The result of this study on GRB 170114A is a polarization degree of 24% throughout the GRB, while the polarization angle of the first time bin is 116° and that of the second time bin is 11°, with χ^2 and number of degrees of freedom (NDF) values of 59.6 and 55, respectively. The resulting $\Delta\chi^2$ map for the first time bin is shown in Supplementary Fig. 11. The $\Delta\chi^2$ map of the second time bin is the same as this but shifted along the polarization angle axis. The results exclude an unpolarized flux with a 99.2% confidence level.

The statistics for this GRB allow the peak to be divided into 3 time bins, each of 2 s. Using these 3 time bins, the same analysis results in a polarization degree of 28%, with a polarization angle of 98° for the first time bin, a polarization angle of 152° for the second time bin and a polarization angle of 38° for the final time bin. The χ^2 and NDF values for this analysis are 27.6 and 29. Note that the number of bins in the modulation curves is reduced here to allow for sufficient statistics in each bin. The final result in the form of a $\Delta\chi^2$ map for the first time bin is shown in Supplementary Fig. 12. This analysis results in a higher exclusion level with a polarization degree of 28%, with a 1σ error of 9%, and excludes an unpolarized flux with 99.7% confidence.

Data availability

All data that support the plots within this paper and other findings of this study are available from the POLAR Collaboration (merlin.kole@unige.ch) upon reasonable request.

Received: 24 July 2018; Accepted: 8 November 2018;
Published online: 14 January 2019

References

1. Woosley, S. E. Gamma-ray bursts from stellar mass accretion disks around black holes. *Astrophys. J.* **405**, 273–277 (1993).
2. Iwamoto, K. et al. A hypernova model for the supernova associated with the γ-ray burst of 25 April 1998. *Nature* **395**, 672–674 (1998).
3. MacFadyen, A. I. & Woosley, S. E. Collapsars: gamma-ray bursts and explosions in 'failed supernovae'. *Astrophys. J.* **524**, 262–289 (1999).
4. Gehrels, N. & Razzaque, S. Gamma-ray bursts in the Swift–Fermi era. *Front. Phys.* **8**, 661–678 (2013).
5. Toma, K. et al. Statistical properties of gamma-ray burst polarization. *Astrophys. J.* **698**, 1042–1054 (2009).
6. Covino, S. & Götz, D. Polarization of prompt and afterglow emission of gamma-ray bursts. *Astron. Astrophys. Trans.* **29**, 205–239 (2016).
7. McConnel, M. High energy polarimetry of prompt GRB emission. *New Astr. Rev.* **76**, 1–21 (2017).
8. Lowell, A. W. et al. Polarimetric analysis of the long duration gamma-ray burst GRB 160530A with the balloon borne Compton Spectrometer and Imager. *Astrophys. J. Lett.* **848**, 119–129 (2017).
9. Yonetoku, D. et al. Magnetic structures in gamma-ray burst jets probed by gamma-ray polarization. *Astrophys. J. Lett.* **758**, L1 (2012).
10. Yonetoku, D. et al. Detection of gamma-ray polarization in prompt emission of GRB 100826A. *Astrophys. J. Lett.* **743**, L30 (2011).
11. Produit, N. et al. Design and construction of the POLAR detector. *Nucl. Instrum. Methods Phys. Res. A* **877**, 259–268 (2018).
12. Li, Z. H. et al. In-orbit instrument performance study and calibration for POLAR polarization measurements. *Nucl. Instrum. Methods Phys. Res. A* **900**, 8–24 (2018).
13. Kole, M. et al. Instrument performance and simulation verification of the POLAR detector. *Nucl. Instrum. Methods Phys. Res. A* **872**, 28–40 (2017).
14. Koshut, T. M. et al. T_{90} as a measurement of the duration of GRBs. *186th AAS Meeting of the Bulletin of the American Astronomical Society* 886 (Conference Series Volume 27, American Astronomical Society, 1995).
15. Maier, D., Tenzer, C. & Santangelo, A. Point and interval estimation on the degree and the angle of polarization: a Bayesian approach. *Publ. Astron. Soc. Pac.* **126**, 459–468 (2014).
16. Westfold, K. C. The polarization of synchrotron radiation. *Astrophys. J.* **130**, 241–258 (1959).
17. McMaster, W. H. Matrix representation of polarization. *Rev. Mod. Phys.* **33**, 8–28 (1961).
18. Lazzati, D., Rossi, E., Ghisellini, G. & Rees, M. J. Compton drag as a mechanism for very high linear polarization in gamma-ray bursts. *Mon. Not. R. Astron. Soc.* **347**, L1–L5 (2004).
19. Granot, J. The most probable cause for the high gamma-ray polarization in GRB 021206. *Astrophys. J. Lett.* **596**, L17–L21 (2003).
20. Lan, M. X., Wu, X. F. & Dai, Z. G. Gamma-ray burst optical afterglows with two-component jets: polarization evolution revisited. *Astrophys. J.* **860**, 44–51 (2018).
21. Rossi, E. M., Lazzati, D., Salmonson, J. D. & Ghisellini, G. The polarization of afterglow emission reveals gamma-ray bursts jet structure. *Mon. Not. R. Astron. Soc.* **354**, 86–100 (2004).
22. Gill, R. & Granot, J. Afterglow imaging and polarization of misaligned structured GRB jets and cocoons: breaking the degeneracy in GRB 170817A. *Mon. Not. R. Astron. Soc.* **478**, 4128–4141 (2018).
23. Rees, M. J. & Meszaros, P. Unsteady outflow models for cosmological gamma-ray bursts. *Astrophys. J. Lett.* **430**, L93–L96 (1994).

24. Paczynski, B. & Xu, G. Neutrino bursts from gamma-ray bursts. *Astrophys. J.* **427**, 708–713 (1994).
25. Mészáros, P. & Rees, M. J. Steep slopes and preferred breaks in gamma-ray burst spectra: the role of photospheres and comptonization. *Astrophys. J.* **530**, 292–298 (2000).
26. Rees, M. J. & Mészáros, P. Dissipative photosphere models of gamma-ray bursts and X-ray flashes. *Astrophys. J.* **628**, 847–852 (2005).
27. Zhang, B. & Yan, H. The internal-collision-induced magnetic reconnection and turbulence (ICMART) model of gamma-ray bursts. *Astrophys. J.* **726**, 90–113 (2011).
28. Lundman, C., Vurm, I. & Beloborodov, A. M. Polarization of gamma-ray bursts in the dissipative photosphere model. *Astrophys. J.* **856**, 145 (2018).
29. Deng, W., Zhang, H., Zhang, B. & Li, H. Collision-induced magnetic reconnection and a unified interpretation of polarization properties of GRBs and blazars. *Astrophys. J. Lett.* **821**, L12–L19 (2016).
30. Xiong, S. L. et al. Overview of the GRB observation by POLAR. In *35th International Cosmic Ray Conference* 640 (Proceedings of Science, 2017).
31. Band, D. et al. BATSE observations of gamma-ray burst spectra. I—spectral diversity. *Astrophys. J.* **413**, 281–292 (1993).
32. Avni, Y. Energy spectra of X-ray clusters of galaxies. *Astrophys. J.* **210**, 642–646 (1976).
33. *GCN Circular: GRB 170114A: Fermi GBM Detection* (2015); https://gcn.gsfc.nasa.gov/other/170114A.gcn3

Acknowledgements

We gratefully acknowledge financial support from the National Basic Research Program (973 Program) of China (grant number 2014CB845800); Joint Research Fund in Astronomy, under cooperative agreement between the National Natural Science Foundation of China and Chinese Academy of Sciences (grant number U1631242); National Natural Science Foundation of China (grant numbers 11503028 and 11403028); Strategic Priority Research Program of the Chinese Academy of Sciences (grant number XDB23040400); Swiss Space Office of the State Secretariat for Education, Research and Innovation (ESA PRODEX Programme); National Science Center of Poland (grant number 2015/17/N/ST9/03556); and Youth Innovation Promotion Association of the Chinese Academy of Sciences (grant number 2014009). We also thank J. M. Burgess of MPE, Garching, Germany, for providing the energy spectra for GRB 170114A.

Author contributions

T.-W.B., T.Batsch, T.Bernasconi, F.C., J.-Y.C., Y.-W.D., N.G., W.H., M.K., H.-C.L., L.L., Z.-H.L., J.-T.L., X.L., R.M., S.O., M.P., N.P., D.R., H.-L.S., L.-M.S., J.-C.S., J.S., T.T., R.-J.W., X.Wen, B.-B.W., X.Wu, H.-L.X., S.-L.X., L.-Y.Z., L.Z., S.-N.Z., X.-F.Z., Y.-J.Z. and A.Z. contributed to the development of the mission concept and/or construction and testing of POLAR. M.K., Z.-H.L., N.P., J.-C.S., Y.-H.W., S.-L.X. and S.-N.Z. were involved in the presented analysis. Z.-G.D., M.-X.L. and X.-F.W. contributed to the theoretical discussions. The manuscript was produced by M.K., Z.-H.L., J.-C.S., Y.-H.W. and S.-N.Z. The principal investigators of the POLAR collaboration are S.-N.Z., M.P. and X.Wu.

Competing interests

The authors declare no competing interests.

Additional information

Supplementary information is available for this paper at https://doi.org/10.1038/s41550-018-0664-0.

Reprints and permissions information is available at www.nature.com/reprints.

Correspondence and requests for materials should be addressed to S.-N.Z. or M.K.

Publisher's note: Springer Nature remains neutral with regard to jurisdictional claims in published maps and institutional affiliations.